Ebulliometric Method for Measuring Activity Coefficients at Infinite Dilution: Systems with Cyclic Ethers

Katherine A. Pividal and Stanley I. Sandler*

Department of Chemical Engineering, University of Delaware, Newark, Delaware 19716

Comparative ebulliometry was used to measure activity coefficients at infinite dilution for the binary systems tetrahydrofuran separately with cyclohexane, ethyl acetate, *n*-pentane, *n*-hexane, and *n*-heptane, cyclohexane with ethyl acetate, 1,4-dioxane with *n*-heptane, and 2-furaldehyde with butyl ether. To correct for differences between the composition of the feed solution and the actual liquid equilibrium composition, the evaporation factor was measured. Parameters for several Gibbs free energy models were determined from the activity coefficients at infinite dilution, and the predictions of the models over the whole composition region were compared with vapor–liquid equilibrium data for some of the systems studied. The experimental results were also compared to UNIFAC predictions.

Introduction

In the absence of reliable experimental vapor–liquid equilibrium data, activity coefficients at infinite dilution can be used to model vapor–liquid equilibrium phase behavior of mixtures. The relative experimental ease and rapid approach to equilibrium make ebulliometry a preferred method of measuring activity coefficients at infinite dilution (*1–3*). Parameters of local composition activity coefficient models such as Wilson, NRTL, or UNIQUAC can be determined directly from activity coefficients at infinite dilution. Infinite dilution activity coefficients themselves are important in separation techniques for very dilute systems, such as the production of high-purity reagents and the separation of pollutants from the environment. Since activity coefficients at infinite dilution represent the maximum deviation from ideal solution behavior for most binary systems, model parameters determined from activity coefficients at infinite dilution can be used to accurately predict vapor–liquid equilibrium throughout the composition range. However, if an activity coefficient model has little or no theoretical basis, predictions based on activity coefficients at infinite dilution may not be optimal.

Group contribution methods, such as UNIFAC (*4*) and TOM (*5*), may be used for predicting activity coefficients and other thermodynamic properties of liquid mixtures, when no experimental data are available. However, the UNIFAC group-interaction parameter table is only about 50% complete so there is a need for the evaluation of the missing parameters. Activity coefficients at infinite dilution provide information to estimate these missing group-interaction parameters (*6*). Also the infinite dilution region provides an especially severe test of the UNIFAC method which is known to give questionable predictions of infinite dilution activity coefficients, especially for mixtures of molecules of very different size (*7*, *8*).

Theory

Comparative ebulliometry for determining activity coefficients at infinite dilution consists of measuring the boiling temperature at constant pressure or the equilibrium pressure at constant temperature of binary mixtures as a function of gravimetrically prepared composition. By using twin ebulliometers, one a reference ebulliometer containing only the pure solvent, temperature differences can be measured directly thereby reducing the error that would be obtained in determining the temperature difference by measuring two absolute temperatures. Using the equilibrium relation $f_i^L = f_i^V$, where f_i is the fugacity of species i, Gautreaux and Coates (*9*) derived the equations to determine activity coefficients at infinite dilution from these measurements without any assumptions concerning the ideality of the liquid or gas phase.

At low pressures, the isobaric experiment is preferred because it is easier to perform. The equation for the activity coefficient at infinite dilution derived by Dohnal and Novotná (*10*) is

$$\gamma_1^\infty = \frac{\epsilon_1^\infty P_2^{sat}}{P_1^{sat}}\left[1 - \beta\frac{d\ln P_2^{sat}}{dT}\left(\frac{\partial T}{\partial x_1}\right)_P^{x_1\to 0}\right] \quad (1)$$

where

$$\epsilon_1^\infty = \exp\left[\frac{(B_{11} - v_1^L)(P_2^{sat} - P_1^{sat}) + \delta_{12}P_2^{sat}}{RT}\right]$$

$$\beta = 1 + P_2^{sat}\left(\frac{B_{22} - v_2^L}{RT}\right)$$

$$\delta_{12} = 2B_{12} - B_{11} - B_{22}$$

where B_{ii} and B_{ij} are second virial coefficients for like and unlike species, respectively, P_i^{sat} is the pure component vapor pressure, and v_i^L is the liquid molar volume of component i. This equation makes no assumption regarding the liquid-phase ideality but uses a truncated virial equation of state to model the vapor phase. Experimental ebulliometric data can be used to determine $(\partial T/\partial x_1)_P^{x_1\to 0}$, the limiting slope at infinite dilution.

One problem that arises in the measurements is that the solution charged into the ebulliometer of known gravimetrically prepared composition is not the liquid composition in equilibrium in the cell. This is because this solution splits into a liquid and vapor phase, with each phase having a different composition from that of the feed. A correction, the evaporation factor (f), accounts for this difference in composition. The evaporation factor is defined to be

$$f = \frac{N_v + N_V^{VLE}}{N_L^{VLE}} \quad (2)$$

where N_L^{VLE} and N_V^{VLE} are the moles of liquid and vapor in equilibrium and N_V is the moles of condensed vapor holdup not yet returned to the boiling chamber. From a mass balance around the ebulliometer we can show that

$$f = \frac{z_i - x_i}{K_i x_i - z_i} \quad (3)$$

or

$$x_i = z_i\left(\frac{1 + f}{1 + K_i f}\right) \quad (4)$$

0021-9568/88/1733-0438$01.50/0

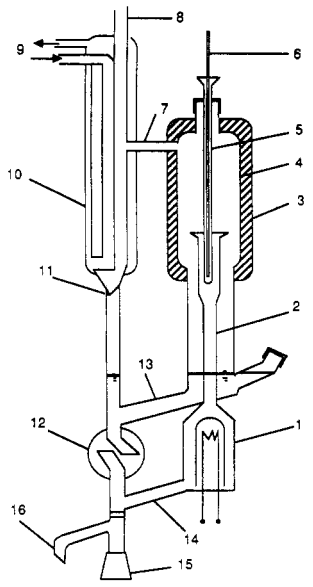

Figure 1. Schematic diagram of the ebulliometer: (1) still pot, (2) Cottrell pump, (3) insulation, (4) VLE chamber, (5) thermowell, (6) thermocouple, (7) vapor passover, (8) to pressure controller, (9) coolant inlet and outlet, (10) condenser, (11) condenser vapor drop, (12) mixing chamber, (13) and (14) liquid recycle, (15) stopcock, and (16) drain port.

Equation 3 was used to determine the evaporation factors from gravimetrically prepared compositions (z_i) and measured liquid compositions (x_i), while eq 4 is used once the evaporation factor is known to correct experimental data for the difference z_i and x_i.

Equipment and Procedure

Twin ebulliometers of the type shown in Figure 1 have been set up recently in cooperation with the Technical University of Berlin. The ebulliometers are connected though a common manifold to a high-accuracy Texas Instruments Heise PPC159 precision pressure controller and measuring system. Pressure is controlled to ±0.001 kPa and measured to ±0.01 kPa absolute. The difference in boiling temperatures of the fluids in both ebulliometers are measured with differential platinum resistance thermometers read with an AB S 1220 series digital readout manufactured by Systemtechnik of Sweden. The differential and absolute temperature are measured to ±0.001 and to ±0.010 °C, respectively, with this equipment.

The details of the glass ebulliometer used for this research and the schematic of the entire apparatus and support equipment are shown in Figures 1 and 2, respectively. The operation of the ebulliometers is based on the principle of the Cottrell vapor lift pump, which enhances the vapor–liquid contact and decreases the time required to approach equilibrium. The boiling chamber, surrounded completely by a heating element, contains less than 10 mL of fluid. The heating finger and walls of the boiling chamber contain fused glass beads, enhancing nucleation and increasing the heated surface-to-volume ratio, which produces smooth and continuous boiling for most fluids. The design of the ebulliometer ensures that the boiling solution recycling through the ebulliometer is well mixed and that the evaporation factor is small.

Aldrich HPLC grade chemicals were used in all experiments. As received, *n*-hexane, *n*-pentane, and 2-furaldehyde were at 98+% purity; these were purified further in a reduced-pressure glass distillation column with 12 stages. After purification all materials used had a purity of better than 99.9% as determined by gas chromatography, except *n*-hexane, which could only be purified to 99.3%, and 2-furaldehyde, which due to oxidation could only be purified to 99.5 mol %. The major impurities in the *n*-hexane were hexane isomers. Pure component vapor

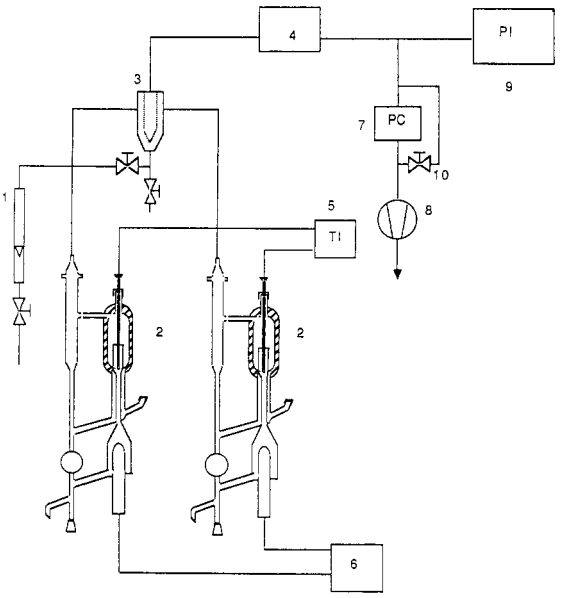

Figure 2. Experimental setup and support equipment for comparative ebulliometry: (1) flow indicator for the nitrogen purge, (2) twin ebulliometers, (3) cold trap, (4) 50-L buffer volume, (5) thermocouple and digital readout, (6) heating units, (7) pressure indicator and controller, (8) vacuum pump, (9) pressure indicator, and (10) valve.

Table I. Measured Vapor Pressures Compared to Literature Values and Coefficients of the Antoine Equation[a]

component	T, °C	P^{sat}, kPa exptl	P^{sat}, kPa lit.[b]	A	B	C
tetrahydrofuran	40.0	40.153	40.224	6.44103	1384.211	246.153
	60.0	83.129	83.172			
cyclohexane	40.0	24.618	24.623	6.15159	1301.696	233.445
	60.0	51.964	51.886			
n-pentane	40.0	115.42	115.65	6.69732	1482.01	279.740
n-hexane	40.0	37.250	37.253	6.13706	1245.97	232.883
	60.0	76.375	76.356			
n-heptane	40.0	12.232	12.243	5.90875	1196.680	208.230
	60.0	27.983	28.043			
	80.0	56.969	57.028			
ethyl acetate	40.0	25.056	25.043	6.22439	1243.969	217.792
	60.0	55.761	55.723			
1,4-dioxane	40.0	10.103	10.132	6.56014	1556.983	240.566
	60.0	23.892	23.987			
	80.0	50.625	50.485			
2-furaldehyde	95.0	10.750	11.279	5.58132	1138.984	155.741
	115.0	23.699	24.331			
butyl ether	95.0	22.924	23.303	6.3620	1578.98	220.947
	115.0	45.864	46.092			

[a] $\log P^{sat}$ (kPa) = $A - B/T$ (°C) + C. [b] From Boublík, Freid, and Halá (*11*).

pressures were measured as a further test of purity and these appear in Table I.

The ebulliometers were cleaned with distilled water, rinsed with HPLC grade acetone, and subjected to total evacuation for at least 4 h before starting an experiment. The ebulliometer system, including the 50-L buffer volume used to reduce pressure fluctuations, was purged with grade 5 nitrogen (99.999%) twice and then brought to the desired pressure. The reference ebulliometer was charged with about 40 mL of solvent by using either a disposible or a glass syringe depending on the nature of the solvent. Forty milliliters of the solvent were then carefully weighed into the second ebulliometer using a Mettler AE 163 balance, as were later additions of solute. Weights of solute and solvent are accurate to ±0.01 and ±0.1 mg, respectively. The solvent was then heated slowly in the ebulliometers, each controlled by separate Variacs. Once boiling started and equilibrium was achieved, the vapor pressure of the solvent was measured and then compared to data in the literature. For these and other measurements, the drop rate from the condenser was maintained between 120 and 140 drops/min, as this was found to produce good pure component vapor pres-

sure data and, for mixtures, the *f* factor was found to be approximately independent of boiling rate in this range.

Once the desired temperature was achieved by adjusting the pressure controller, a small quantity of the solute (~5 μL) was weighed in a pressure lock syringe and injected into one of the ebulliometers. The temperature difference between the two ebulliometers was recorded after equilibrium had again been achieved. Then an additional quantity of weighed solute, approximately twice the amount of the previous injection, was added to the ebulliometer. The procedure of adding solute was repeated until the solute concentration in the ebulliometer was between 0.03 and 0.04 mole fraction. The isobaric limiting slope $(\partial T/\partial x_1)_P^{x_1 \to 0}$ could then be found by fitting the change in temperature to a second-order polynomial in the composition of the equilibrium liquid solution after using the evaporation factor correction.

The *f* factor was measured by charging the ebulliometer with a solution of known composition, which was also used in the calibration of the gas chromatograph. After equilibrium was achieved, a 0.5-μL sample of the boiling liquid was drawn from the sample port and the composition was determined by gas chromatography (5730A Hewlett Packard gas chromatograph and a Hewlett Packard 390A integrator). Once the feed composition, equilibrium liquid composition, and the relative volatility of the solution was known, the *f* factor is determined by using eq 3. Since the relative volatility is, in general, not known before the experiments, this calculation must be done iteratively as described below.

Data Analysis and Results

For the calculation of the *f* factor from eq 3, the *K* factor ($K_i = y_i/x_i$) was needed. Here, the K_i was estimated from an activity coefficient model whose parameters where derived from measured activity coefficients at infinite dilution by using a procedure to be described shortly. However, it should be noted that significant differences in the feed and equilibrium liquid composition were only apparent in solutions whose relative volatilities were greater than two.

In Figures 3, examples of the change in temperature as a function of the liquid mole fraction charged are shown. Experimental data are used to determine the limiting slope by fitting the data to the second degree polynomial

$$\Delta T = ax_i + bx_i^2 \qquad (5)$$

assuming that the feed and equilibrium liquid compositions were identical. The limiting slope $(\partial T/\partial x_i)_P^{x_1 \to 0}$ was determined from the value of *a*. [Data were also fit to first and third degree polynomials, and since the data are approximately linear, the limiting slopes using different order polynomials gave γ_i^∞ which differed by less than 5%. The use of higher order polynomials did not give significant improvements in the standard deviation to that obtained by using a second-order polynomial fit.] Next, the limiting slopes were used in eq 1 to estimate the activity coefficients at infinite dilution, which were then used to estimate the parameters in the two-suffix Margules, van Laar, Wilson, NRTL, and UNIQUAC equations. The *K* factor was then determined for each feed composition by using the activity coefficient model and the vapor pressure data, and using eq 3, the *f* factor was calculated. This *f* factor was used to correct the liquid compositions at each data point by using eq 4. From the corrected liquid compositions and the measured change in temperature, new activity coefficients at infinite dilution were determined. This calculation procedure was repeated until the calculation converged. In these calculations the measured pure component vapor pressures were used, and the vapor-phase nonidealities at low pressure were accounted for by using a truncated virial equation of state. The generalized method of

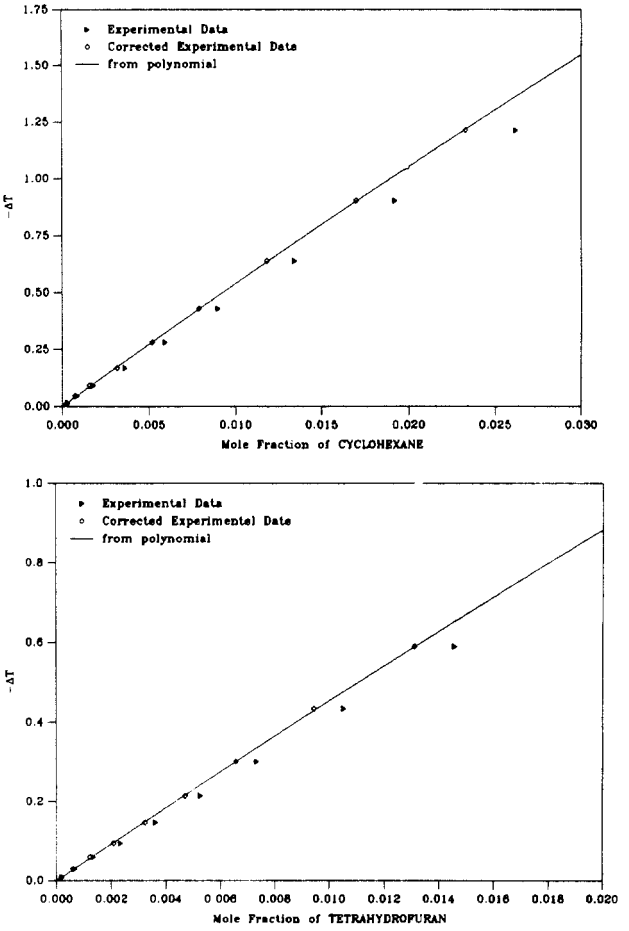

Figure 3. ΔT as a function of feed composition (▶) and equilibrium liquid composition (◇) and the second-order polynomial fit from which the limiting slopes is found for the system ethyl acetate/cyclohexane at 40.0 °C.

Hayden and O'Connell (*11*) was used to determine these second virial coefficients; other pure component data were taken primarily from Reid et al. (*12*) and Boublík et al. (*13*).

The *f* factor so determined ranged from 0.05 to 0.075, depending on the temperature and on the species used. The values are given in Table II. Since the overall effect of the evaporation factor is small, and most of the values for this parameter clustered around 0.06, this value was used for all further calculations. Even so, the equilibrium liquid compositions had to be determined from the prepared feed by iteration since $K_i = y_i/x_i$ is unknown. The calculational procedure followed is indicated in the flow chart of Figure 4. Figures 3 also contain an example of the data for $-\Delta T$ as a function of the corrected compositions (denoted by the points ◇) and the polynomial fits of these data.

The calculated activity coefficients at infinite dilution and corresponding limiting slope $(\partial T/\partial x_1)_P^{x_1 \to 0}$ are given in Table III. Experimental errors inherent in the apparatus used are 0.02 and 0.1 mg for each measurement of solute and solvent made, and 0.0025 °C for each differential temperature measurement. The major source of error encountered in these type of measurements comes from not knowing the exact *f* factor. Experiments of the type used for Table II have shown that the *f* factor varies between 0.05 and 0.07 depending on the condensation drop rate, pressure, temperature, and composition. In the calculation of the error in the measurement of the limiting slope, an error of ±0.01 was used for the *f* factor. The results of the error analysis on both limiting slopes and activity coefficients at infinite dilution are given in Table III. At relative volatilities greater than 2, the most significant error in the activity coefficients at infinite dilution is due to the *f* factor; this error

Table II. Measured *f* Factor Compared to Drop Rate for the Binary System 1,4-Dioxane (1)/Heptane (2)

For z_1 = 0.02298 (Feed Composition), Run 1

T, °C	drop rate, drops/min	x_1 at equilib	$K_1(y_1/x_1)$	*f* factor
78.500	60	0.0220	2.2	0.039
78.511	88	0.0218	2.2	0.047
78.537	128	0.0213	2.2	0.070
78.541	152	0.0211	2.2	0.079
58.709	60	0.0219	2.6	0.033
58.736	92	0.0216	2.6	0.043
58.756	120	0.0215	2.6	0.046
58.761	132	0.0213	2.6	0.053
58.767	156	0.0214	2.6	0.050
58.792	200+	0.0211	2.6	0.060

For z_2 = 0.02509 (Feed Composition), Run 2

T, °C	drop rate, drops/min	x_2 at equilib	$K_2(y_2/x_2)$	*f* factor
78.023	44	0.0232	3.8	0.030
78.025	68	0.0229	3.8	0.035
78.036	92	0.0225	3.8	0.042
78.060	112	0.0220	3.8	0.052
78.089	124	0.0220	3.8	0.058
78.111	152	0.0217	3.8	0.058
57.935	56	0.0209	4.7	0.057
57.982	80	0.0208	4.7	0.059
58.003	112	0.0201	4.8	0.071
57.989	144	0.0202	4.8	0.069
57.991	168	0.0202	4.8	0.069
58.004	192	0.0202	4.8	0.069

becomes unacceptable only when the relative volatility is larger than 10. The error analysis shows that the next major uncertainty in the experiment is the measurement of the temperature difference, especially when the temperature difference is small (i.e., $|(\partial T/\partial x_i)_P^{x_i \to 0}| \leq 10$). In one case the error was as large as 40% (see Table III for γ_2^∞ and $(\partial T/\partial x_2)_P^{x_2 \to 0}$ of tetrahydrofuran in cyclohexane) though this translated to an uncertainty in the activity coefficients at infinite dilution of less than 2%. The determination of activity coefficients at infinite dilution greater than 5 resulted in the largest errors, though these were less than 6%. On the average, the deviation in measured activity coefficients at infinite dilution was less than 2% for the systems studied here.

The two-suffix Margules, van Laar, Wilson, NRTL, and UNIQUAC activity coefficient models were used to estimate vapor–liquid equilibrium over the entire composition range, and to estimate relative volatilities of solutions in the ebulliometer for the *f* factor determination. The model parameters of the Wilson, NRTL, and UNIQUAC activity coefficient models were determined by a Newton–Raphson iteration, while Margules and van Laar model parameters were determined directly from γ_1^∞ and γ_2^∞. The relative volatilities calculated for the five activity

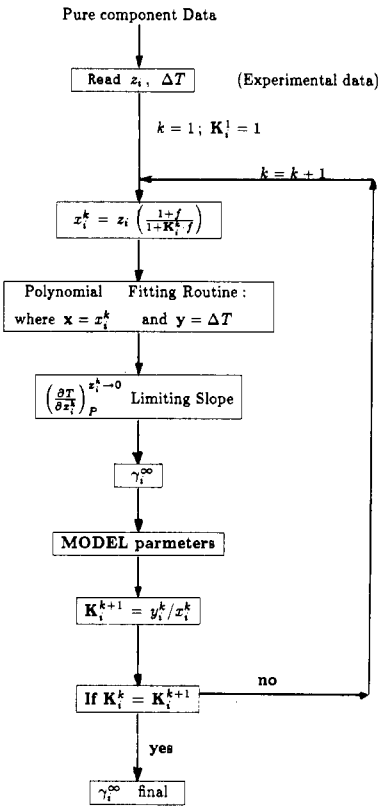

Figure 4. Flow diagram for the calculation of γ_i^∞ from experimental binary and pure component data.

coefficient models for solute compositions less than 0.05 differed by less than 2%. In the mid-composition range, between 0.2 and 0.8 mole fraction, the differences in the pressure/composition predictions of the different models, using model parameters determined at infinite dilution, became more apparent.

The activity coefficients at infinite dilution for tetrahydrofuran separately with *n*-hexane, ethyl acetate, and cyclohexane, for ethyl acetate with cyclohexane (at 40 and 60 °C), and for butyl ether with 2-furaldehyde (at 95 and 115 °C), were measured to compare with the vapor–liquid equilibrium data over the whole composition range taken by Wu and Sandler (*14*). The comparison of the predicted *P*–*x*–*y* diagram (at the 40 °C isotherm), using two-suffix Margules, van Laar, Wilson, NRTL, or UNIQUAC equations with parameters estimated from activity coefficients at infinite dilution, with the experimental data of Wu and Sandler (*14*) are given in Figures 5–9. These figures indicate that all the activity coefficient models give similar predictions of the vapor–liquid equilibrium data. Activity coefficients are plotted versus composition in Figures 10–13 for four sys-

Table III. Measured Activity Coefficients at Infinite Dilution and Limiting Slope

component 1 in component 2	temp, °C	γ_1^∞	$(\partial T/\partial x_1)_P^{x_1 \to 0}$	γ_2^∞	$(\partial T/\partial x_2)_P^{x_2 \to 0}$
tetrahydrofuran/cyclohexane	40.0	1.72 ± 0.02	−46.6 ± 1.0	1.76 ± 0.02	−2.26 ± 0.35
	60.0	1.63 ± 0.02	−46.3 ± 0.9	1.65 ± 0.03	−1.23 ± 0.50
tetrahydrofuran/pentane	40.0	2.19 ± 0.03	6.92 ± 0.38	2.04 ± 0.06	−122.0 ± 4.5
tetrahydrofuran/*n*-hexane	40.0	1.73 ± 0.02	−22.8 ± 0.4	1.95 ± 0.03	−21.2 ± 0.8
	60.0	1.58 ± 0.01	−22.0 ± 0.4	1.82 ± 0.02	−20.2 ± 0.4
tetrahydrofuran/*n*-heptane	40.0	1.79 ± 0.05	−108.8 ± 3.5	2.02 ± 0.09	9.61 ± 0.71
	60.0	1.43 ± 0.03	−84.7 ± 2.2	1.79 ± 0.06	11.4 ± 0.6
tetrahydrofuran/ethyl acetate	40.0	1.09 ± 0.01	−17.0 ± 0.5	1.10 ± 0.03	8.11 ± 0.5
	60.0	1.10 ± 0.01	−16.9 ± 0.5	1.10 ± 0.03	7.75 ± 0.5
ethyl acetate/cyclohexane	40.0	3.33 ± 0.06	−60.0 ± 1.6	2.82 ± 0.06	−41.4 ± 1.3
	60.0	2.95 ± 0.05	−62.8 ± 1.5	2.56 ± 0.04	−37.9 ± 1.0
1,4-dioxane/*n*-heptane	40.2	3.59 ± 0.05	−45.5 ± 1.0	5.47 ± 0.19	−122.6 ± 4.9
	60.0	3.21 ± 0.04	−47.0 ± 1.0	4.83 ± 0.14	−117.7 ± 4.2
	80.0	2.63 ± 0.03	−41.7 ± 0.7	3.97 ± 0.09	−101.0 ± 3.0
butyl ether/2-furaldehyde	95.0	5.52 ± 0.31	−255 ± 16	4.21 ± 0.04	−28.1 ± 0.6
	115.0	5.50 ± 0.27	−268 ± 14	3.98 ± 0.04	−34.9 ± 0.7

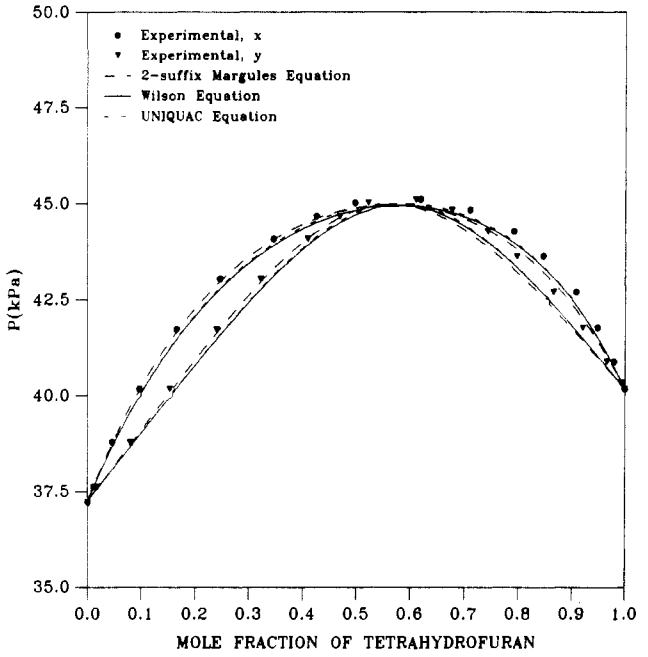

Figure 5. Comparison of predictions of three activity coefficient models with parameters fit to activity coefficients at infinite dilution with experimental vapor–liquid equilibrium data for tetrahydrofuran (1)/*n*-hexane (2) at 40.0 °C of ref *14*.

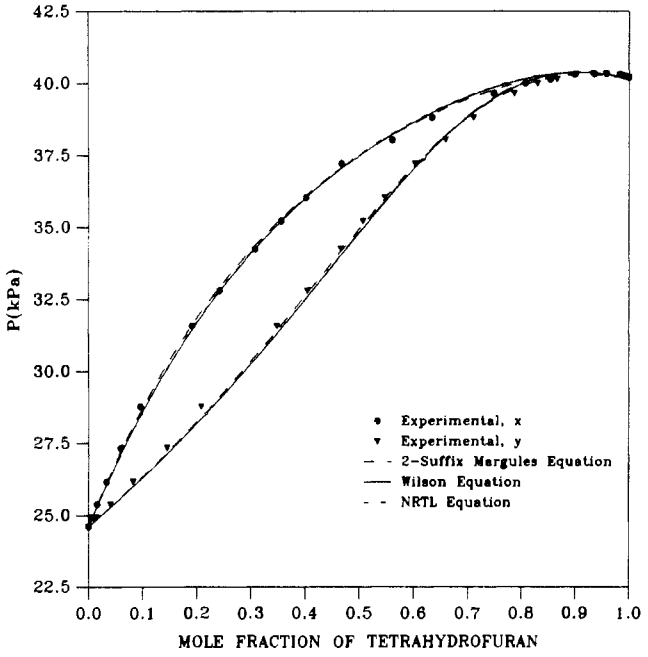

Figure 6. Comparison of predictions of three activity coefficient models with parameters fit to activity coefficients at infinite dilution with experimental vapor–liquid equilibrium data for tetrahydrofuran (1)/cyclohexane (2) at 40.0 °C of ref *14*.

tems which have large activity coefficients at infinite dilution, and for which complete VLE data are available. The NRTL activity coefficient model, which performed best, was used in these figures. The fit of the vapor–liquid equilibrium experimental data to the NRTL model whose parameters were calculated from activity coefficients at infinite dilution was surprisingly good in all cases.

Ternary vapor–liquid equilibrium data were also measured by Wu and Sandler for the system ethyl acetate with cyclohexane and tetrahydrofuran at 40 °C. The results of a comparison of five activity coefficient models with parameters reduced from binary vapor–liquid equilibrium data of Wu and Sandler, and parameters found here from measured activity coefficients at

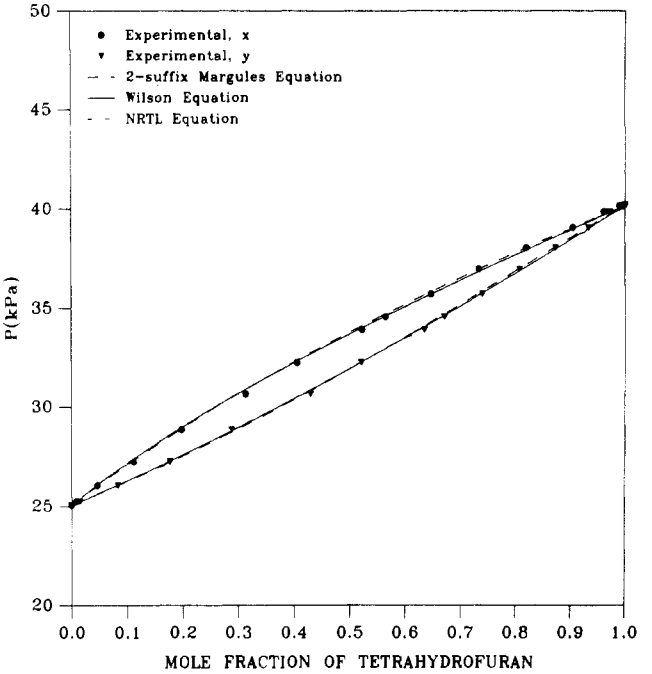

Figure 7. Comparison of predictions of three activity coefficient models with parameters fit to activity coefficients at infinite dilution with experimental vapor–liquid equilibrium data for tetrahydrofuran (1)/ethyl acetate (2) at 40.0 °C of ref *14*.

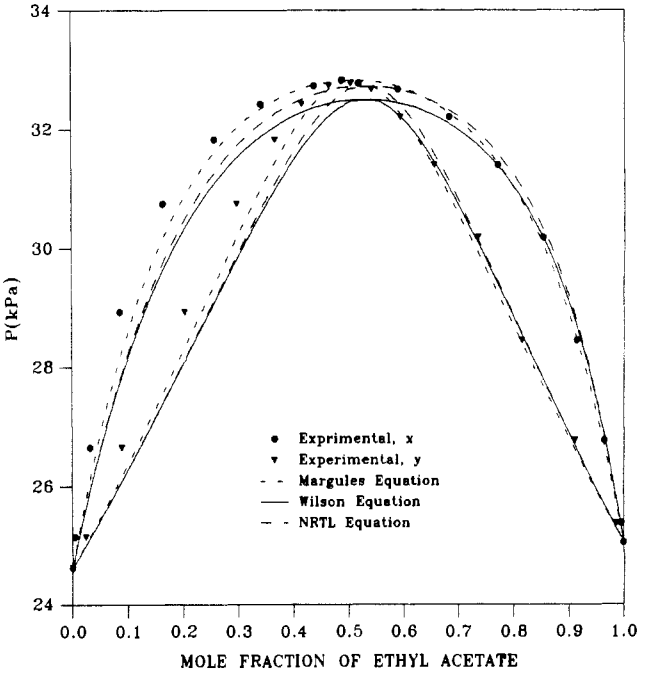

Figure 8. Comparisons of predictions of three activity coefficient models with parameters fit to activity coefficients at infinite dilution with experimental vapor–liquid equilibrium data for ethyl acetate (1)/cyclohexane (2) at 40.0 °C of ref *14*.

infinite dilution given are presented in Table IV. The results show similar agreement in absolute average deviations of the vapor-phase composition and pressure for the Wilson model. However, the other activity coefficient models, while giving slightly better results than the Wilson equation for binary systems, performed less satisfactorily when extended to the ternary system with parameters determined from binary data.

UNIFAC predictions of the infinite dilution activity coefficients are compared to experimental γ_i^∞ in Table V. The UNIFAC method with published parameters (*12*) did not result in accurate predictions of activity coefficients at infinite dilution in most

Table IV. Comparison of the Absolute Average Deviation (AAD) in Pressure and Vapor-Phase Composition of Five Activity Coefficient Models Using Binary Parameters and Experimental Ternary Data[a] for the System Ethyl Acetate (1)/Cyclohexane (2)/Tetrahydrofuran (3) at 40.0 °C

model	parameter[b]	AADy_1	AADy_2	AADy_3	AADP, kPa
Margules	VLE	0.0050	0.0033	0.0061	0.122
	γ^∞	0.0300	0.0260	0.0350	3.114
Van Laar	VLE	0.0053	0.0126	0.0139	0.154
	γ^∞	0.0061	0.0118	0.0140	1.535
Wilson	VLE	0.0039	0.0028	0.0058	0.085
	γ^∞	0.0067	0.0049	0.0074	0.145
NRTL	VLE	0.0039	0.0032	0.0057	0.091
	γ^∞	0.0162	0.0470	0.0389	4.004
UNIQUAC	VLE	0.0087	0.0053	0.0074	0.309
	γ^∞	0.0269	0.0671	0.0454	2.797
UNIFAC		0.0963	0.0479	0.0490	9.805

[a] Ternary data from Wu and Sandler (*14*). [b] Model parameters derived from thermodynamically consistent vapor–liquid equilibrium data (VLE) and activity coefficients at infinite dilution (γ^∞). AAD = absolute average deviation.

of the systems measured. Also shown in Table V are other sources of activity coefficients at infinite dilution: those measured directly by Thomas (*15*) and those predicted from complete VLE data given by Wu and Sandler (*14*) and DECHEMA (*16*) using the Wilson equation. Generally the agreement is quite good.

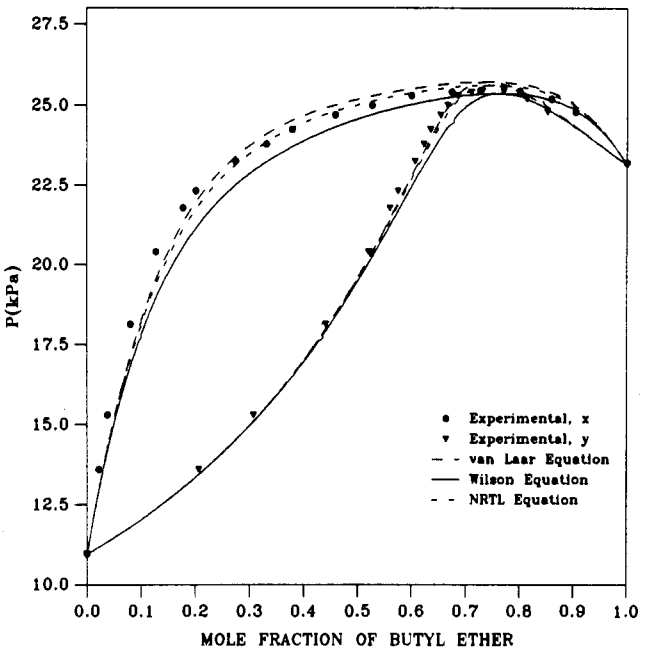

Figure 9. Comparison of predictions of three activity coefficient models with parameters fit to activity coefficients at infinite dilution with experimental vapor–liquid equilibrium data for butyl ether (1)/2-furaldehyde (2) at 95.0 °C of ref *14*.

Conclusions

Comparative ebulliometry was used to measure activity coefficients at infinite dilution for systems containing cyclic ethers. This method of measuring activity coefficients at infinite dilution is accurate and less time consuming than vapor–liquid equilibrium measurements over the entire composition range. It is also shown that, using model parameters derived from measured activity coefficients at infinite dilution, one can accurately predict vapor–liquid equilibrium over the whole composition range. For example, minimum-boiling azeotropes ex-

Table V. Comparison between Measured, Predicted UNIFAC, and Other Sources of Infinite Dilution Activity Coefficients

component 1 in component 2	temp, °C	γ_1^∞ exptl	γ_1^∞ UNIFAC	γ_1^∞ other[a]	γ_1^∞ lit.
tetrahydrofuran/cyclohexane	40.0	1.72	1.314		1.81[b]
	60.0	1.63	1.286		1.70[b]
cyclohexane/tetrahydrofuran	40.0	1.76	1.382	1.69 (55 °C)	1.76[b]
	60.0	1.65	1.351	1.59 (65 °C)	1.61[b]
tetrahydrofuran/*n*-pentane	40.0	2.19	1.361		
n-pentane/tetrahydrofuran	40.0	2.04	1.460		
tetrahydrofuran/*n*-hexane	40.0	1.73	1.288	1.59 (49 °C)	1.75[b]
	60.0	1.58	1.260	1.51 (67 °C)	1.63[b]
n-hexane/tetrahydrofuran	40.0	1.95	1.444		1.94[b]
	60.0	1.82	1.405		1.80[b]
tetrahydrofuran/*n*-heptane	40.0	1.79	1.214		
	60.0	1.43	1.188		
n-heptane/tetrahydrofuran	40.0	2.02	1.399		
	60.0	1.79	1.356		
tetrahydrofuran/ethyl acetate	40.0	1.09	1.132	1.10 (40 °C)	1.13[b]
	60.0	1.10	1.145	1.06 (60 °C)	1.11[b]
ethyl acetate/tetrahydrofuran	40.0	1.10	1.049		1.15[b]
	60.0	1.10	1.098		1.12[b]
ethyl acetate/cyclohexane	40.0	3.33	2.952		3.47[b]
	60.0	2.95	2.803		3.11 (55 °C)[c]
cyclohexane/ethyl acetate	40.0	2.82	3.245		2.93[b]
	60.0	2.56	3.032		2.53 (55 °C)[c]
1,4-dioxane/*n*-heptane	40.0	3.59	2.614		
	60.0	3.21	2.444		
	80.0	2.63	2.304		2.69[c]
n-heptane/1,4-dioxane	40.0	5.47	3.771		
	60.0	4.83	3.496		
	80.0	3.97	3.265		3.78[c]
butyl ether/2-furaldehyde	95.0	5.52	5.302		6.95[b]
	115.0	5.50	5.079		5.53[b]
2-furaldehyde/butyl ether	95.0	4.21	3.399		4.59[b]
	115.0	3.98	3.212		4.08[b]

[a] Infinite dilution activity coefficients measured directly by an ebulliometric method, Thomas (*15*). [b] Infinite dilution activity coefficients estimated from complete VLE data by Wu and Sandler (*14*) using the Wilson equation. [c] Infinite dilution activity coefficients estimated from complete VLE data using the Wilson equation in DECHEMA (*16*).

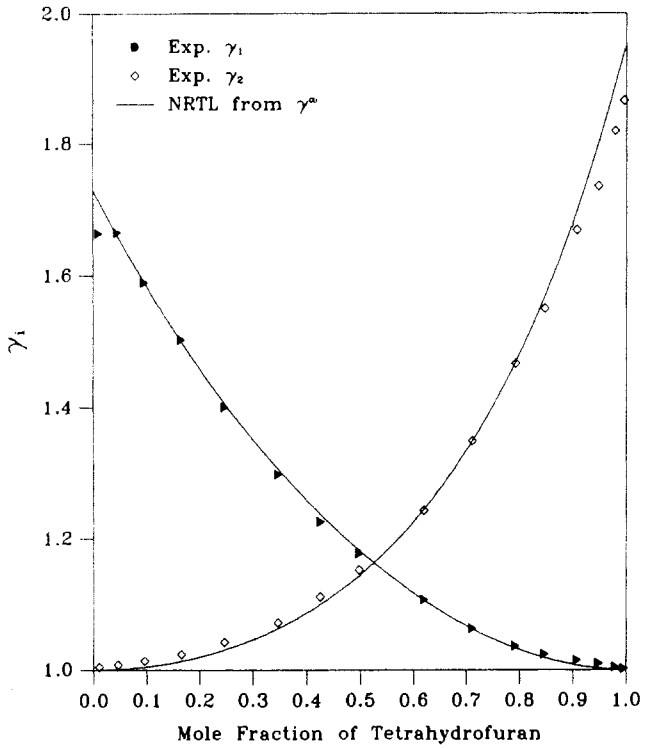

Figure 10. Comparison of predictions of NRTL activity coefficient model with parameters fit to activity coefficients at infinite dilution (lines) with experimental VLE data for (γ_1 (▲) and γ_2 (◇)) for tetrahydrofuran (1)/*n*-hexane (2) at 40 °C from ref *14*.

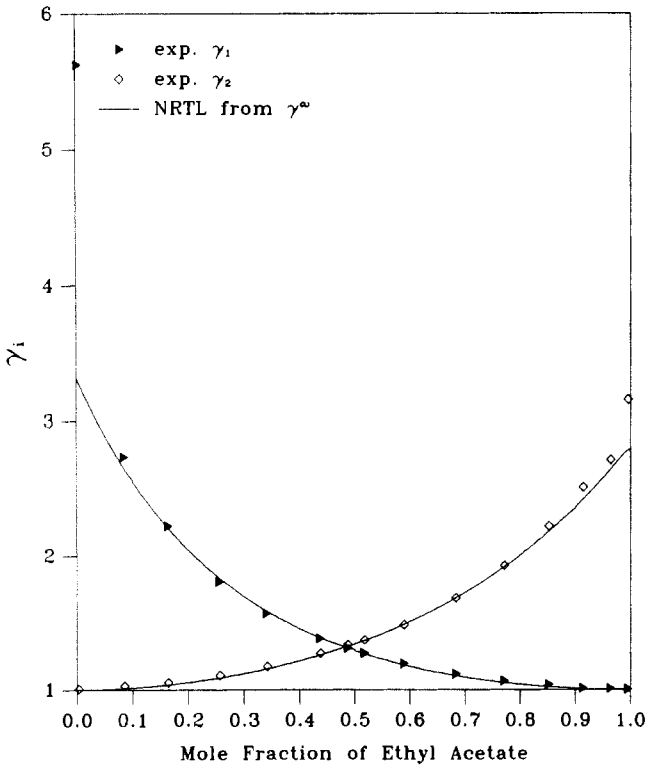

Figure 11. Comparison of predictions of NRTL activity coefficient model with parameters fit to activity coefficients at infinite dilution (lines) with experimental VLE data for (γ_1 (▲) and γ_2 (◇)) for ethyl acetate (1)/cyclohexane (2) at 40 °C from ref *14*.

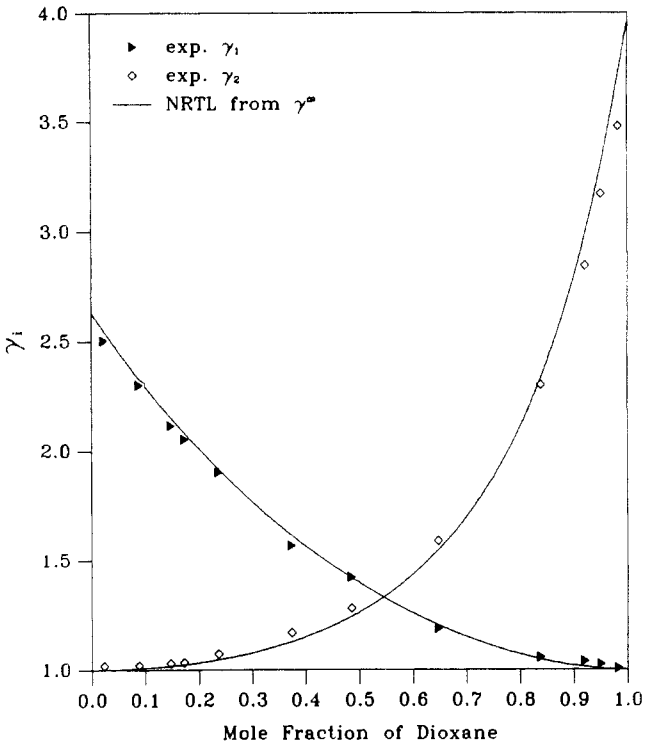

Figure 12. Comparison of predictions of NRTL activity coefficient model with parameters fit to activity coefficients at infinite dilution (lines) with experimental VLE data for (γ_1 (▲) and γ_2 (◇)) for 1,4-dioxane (1)/heptane (2) at 80 °C from ref *16*.

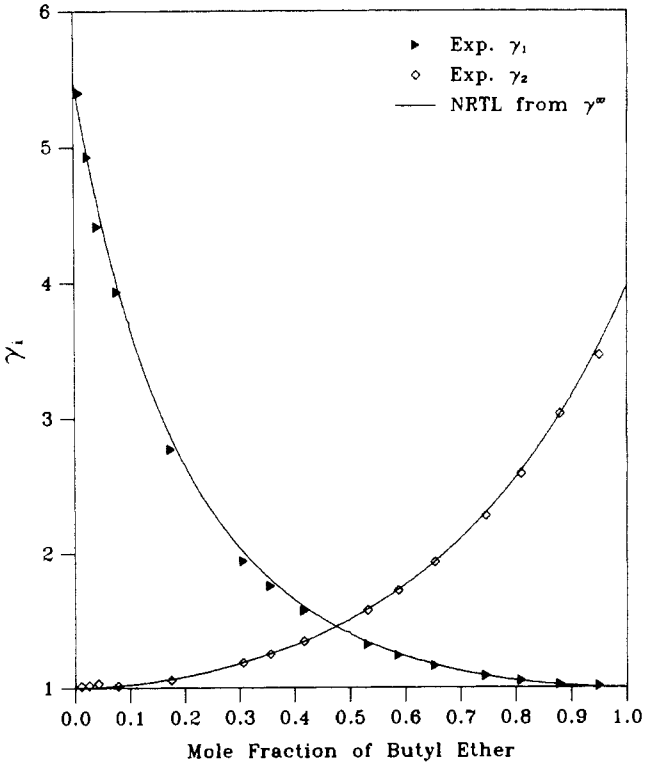

Figure 13. Comparison of predictions of NRTL activity coefficient model with parameters fit to activity coefficients at infinite dilution (lines) with experimental VLE data for (γ_1 (▲) and γ_2 (◇)) for butyl ether (1)/2-furaldehyde (2) at 115 °C from ref *14*.

perimentally observed for the binary systems tetrahydrofuran separately with hexane and cyclohexane, ethyl acetate with cyclohexane, 1,4-dioxane with heptane, and butyl ether with 2-furaldehyde were also found from predictions based on infinite dilution measurements for these systems. Consequently activity coefficients at infinite dilution can be used in engineering design and to estimate interaction parameters of the UNIFAC and

other group contribution methods.

Acknowledgment

Professor Dr. H. Knapp of the Technical University of Berlin (West) supplied us with the ebulliometers used in this work. We are very pleased to acknowledge the assistance of Dr. Ingolf Paul (T. U. B.) and Huey S. Wu (University of Delaware) in setting up this equipment, and their advice.

Glossary

a, b	first- and second-order coefficient of a polynomial least-squares fit
A, B, C	coefficients of the Antoine vapor pressure equation
B_{ii}, B_{ij}	second virial coefficients
f	evaporation factor
f_i^V, f_i^L	fugacity of the liquid and vapor phases for component i
K_i	volatility of component i
N_V	total amount of moles of vapor holdup
N_L^{VLE}, N_V^{VLE}	total moles in liquid and vapor equilibrium phases
P	absolute pressure
P_i^{sat}	saturation vapor pressure of component i
R	gas constant
T	absolute temperature
ΔT	temperature difference
VLE	vapor–liquid equilibrium
v_i^L	liquid molar volume of component i
x	independent variable in least-squares fit
x_i	equilibrium liquid-phase mole fraction of component i
y	dependent variable in least-squares fit
y_i	equilibrium vapor-phase mole fraction of component i
z_i	feed mole fraction component i

Greek Letters

β	$=1 + P_2^{sat}((B_{22} - v_2^L)/RT)$
δ_{12}	$=2B_{12} - B_{11} - B_{22}$
γ_i^∞	activity coefficient at infinite dilution of component i
ϵ_i^∞	vapor-phase correction

Registry No. Tetrahydrofuran, 109-99-9; cyclohexane, 110-82-7; *n*-pentane, 109-66-0; *n*-hexane, 110-54-3; *n*-heptane, 142-82-5; ethyl acetate, 141-78-6; 1,4-dioxane, 123-91-1; 2-furaldehyde, 98-01-1; butyl ether, 142-96-1.

Literature Cited

(1) Dohnal, V.; Bláhová, D.; Holub, R. *Fluid Phase Equilib.* **1982**, *9*, 181.
(2) Eckert, C. A.; Newman, B. A.; Nicolaides, G. L.; Long, T. C. *AIChE J.* **1981**, *27*, 33.
(3) Olson, J. D. *Proc. Eighth Symp. Thermophys. Prop.* **1982**, *1*, 343.
(4) Fredenslund, A.; Gmehling, J.; Rasmussen, P. *Vapor-Liquid Equilibrium Using UNIFAC*; Elsevier: Amsterdam, 1977.
(5) Kehiaian, H. V.; Sandler, S. I. *Fluid Phase Equilib.* **1984**, *17*, 139.
(6) Novotná, M.; Dohnal, V.; Holub, R. *Fluid Phase Equilib.* **1988**, *27*, 373.
(7) Thomas, E. R.; Eckert, C. A. *Ind. Eng. Chem. Process Des. Dev.* **1984**, *23*, 194.
(8) Weidlich, U.; Gmehling, J. *Ind. Eng. Chem. Res.* **1987**, *26*, 1372.
(9) Gautreaux, M. F.; Coates, J. *AIChE J.* **1955**, *1*, 496.
(10) Dohnal, V.; Novotná, M. *Collect. Czech. Chem. Commun.* **1988**, *51*, 1393.
(11) Hayden, J. G.; O'Connell, J. P. *Ind. Eng. Chem. Process Des. Dev.* **1975**, *14*, 209.
(12) Reid, R. C.; Prausnitz, J. M.; Poling, B. E. *The Properties of Gases and Liquids*, 4th ed.; McGraw-Hill: New York, 1986.
(13) Boublík, T.; Fried, V.; Hala, E. *The Vapor Pressures of Pure Substances*; Elsevier: Amsterdam, 1984.
(14) Wu, H.-S.; Sandler, S. I. *J. Chem. Eng. Data* **1988**, *33*, 316.
(15) Thomas, E. R. Ph.D. Thesis, University of Illinois, Urbana, 1980.
(16) Gmehling, J.; Onken, U. *Vapor-Liquid Equilibrium Data Collection*; DECHEMA Chemistry Data Series; DECHEMA: Frankfurt, 1977.

Received for review September 14, 1987. Accepted March 14, 1988. The research reported here was supported, in part, by National Science Foundation Grant CBT-8612285 to the University of Delaware and a grant from the Chevron Oil Field Research Co.

Activity Coefficients in Benzene–Alcohol Systems near the Freezing Point of Benzene

Fernando Aguirre-Ode,* Joel Koo, and Eric Rojas

Departamento de Química, Facultad de Ciencia, Universidad Técnica Federico Santa María, Valparaíso, Chile

Activity coefficients of seven light alcohols and benzene were determined by measuring freezing point depressions of benzene with each alcohol as a solute. Fits to van Laar, Wilson, and some continuous association models showed that the latter models work much better in all cases, considering alcohols as monomeric solutes. This behavior is similar to that observed at much lower temperatures when thiophene is the solvent of butanols. The magnitudes of the association equilibrium constants in the low-concentration range are also much lower than those calculated on the basis of properties of pure alcohols with athermal models of continuous association.

Introduction

Activity coefficients of both components in benzene–alcohol systems were calculated from smoothed freezing point depressions of benzene in a similar manner to that used when either cyclohexane (*1*) or thiophene (*2*) was the solvent. As expected, monomers appeared to be the smallest species at high dilution, the same behavior that was observed when thiophene was the solvent.

A fit to six different solution models showed analogous trends. However, in this study there were indications of difficulties in fitting some particular models, the ones that showed large standard deviations in past reports (*1*, *2*).

Experimental details have been given elsewhere (*1*).

Calculation of Activity Coefficients from Experimental Data

The sequence of calculations is the same as given in a previous paper (*2*). Smoothing of freezing point depressions, θ, is done through

$$\theta = \frac{z[A_0 + (A_1 - 1)z + A_2 z^2]}{A[A_0 + A_1 z + A_2 z^2]} \quad (1)$$

in which $z = x_2/x_1$, the mole fraction ratio

$$A = \lambda_1/RT_0^2 = 0.015418 \quad (2)$$

* To whom correspondence should be addressed.

0021-9568/88/1733-0445$01.50/0